

# A Legendre-Galerkin Spectral Method for Second-Order Elliptic Eigenvalue Problems in a Complex Sectoral Region

Xuechun Mu<sup>1</sup>, Jihui Zheng<sup>1,\*</sup>

<sup>1</sup>School of Mathematics Science, Guizhou Normal University, Guiyang 550025, China

**Abstract**— In this paper, a Legendre-Galerkin spectral method for solving second-order elliptic eigenvalue problems in complex regions is presented. An affine transformation is first constructed to transform the second-order elliptic eigenvalue problem in a complex sectoral region into an equivalent second-order eigenvalue problem in a standard rectangular region. Subsequently, an appropriate Sobolev space is introduced based on the boundary conditions, and the variational and discrete formats of the second-order eigenvalue problem within the standard rectangular domain are derived. The matrix form of the discrete format is then derived using Legendre basis functions and tensor product methods. Finally, the convergence and high accuracy properties of the algorithm are demonstrated through numerical experiments.

**Keywords**— Eigenvalue problem; complex sectoral region; Legendre-Galerkin approximation.

## I. INTRODUCTION

Eigenvalue problems hold profound physical significance and find extensive applications across various scientific and engineering disciplines [1]. Consequently, the development of efficient and accurate numerical methods for solving eigenvalue problems has consistently been an important direction and an active area of research in the academic community. It is well known that when the problem is defined on regular domains, a variety of efficient numerical methods are available, such as the finite element method, finite difference method, and spectral methods. In [5], Shen proposed an efficient and accurate spectral-Galerkin method for biharmonic equation on a unit disk. In [6], An et al. developed a spectral-Galerkin approximation and optimal error estimate for biharmonic eigenvalue problems in circular, spherical, and elliptical domains. In [7], Li et al. developed a spectral approximation based on the orthogonal polynomials on the unit ball. In [8], An et al. Constructed an efficient spectral-Galerkin approximation and error analysis for Maxwell transmission eigenvalue problems in spherical geometries.

Spectral methods have emerged as a principal computational approach for solving partial differential equations (PDEs) [9], demonstrating exceptional accuracy in handling problems with smooth solutions. Nevertheless, their practical implementation remains predominantly constrained to regular geometric configurations; specifically, these techniques are primarily restricted to canonical domains such as intervals, rectangular regions, and cuboidal spaces. This geometric constraint substantially limits their broader applicability across more complex spatial domains. This imperative necessitates the development of high-precision numerical methodologies for nonlinear eigenvalue problems in complex domains. Substantial efforts have been devoted to implementing fictitious domain formulations for PDE solutions in irregular configurations. Notable contributions include the rigorous spectral techniques established by Gu and Shen [13] for elliptic equations in complex geometries, along with Lui's innovative

approach integrating domain embedding strategies for PDE resolution [16]. Seminal work by Orszag [17] further advanced this paradigm through a Fourier-Chebyshev spectral framework employing explicit coordinate transformations to solve annular heat transfer problems. Wang et al. [18] employed a polar coordinate transformation to map the complex domain onto a unit disk, constructed a Fourier-Legendre spectral Galerkin scheme, and analyzed the optimal convergence of the numerical solution, representing a milestone in computational mapping techniques.

To the best of our knowledge, there are relatively few studies on spectral methods for eigenvalue problems in complex sectoral regions. Therefore, this paper aims to propose a Legendre-Galerkin spectral approximation based on a mapping method for second-order eigenvalue problems in complex sectoral regions. Initially, an affine transformation is constructed to map the second-order elliptic eigenvalue problem defined in complex sectoral regions onto an equivalent formulation within a standard rectangular domain. Subsequently, a suitable Sobolev space is defined in accordance with boundary conditions, enabling the derivation of both variational and discrete formulations for the transformed eigenvalue problem. The discrete system is then expressed in matrix form through tensor product expansions using Legendre orthogonal basis functions. Ultimately, numerical experiments are conducted, demonstrating the algorithm's convergence properties and high-order accuracy characteristics.

The remainder of this article is organized as follows. In Section 2, we introduce an appropriate Sobolev space and deduce the weak form and corresponding discrete scheme. In Section 3, we describe in detail the efficient implementation of the algorithm. In Section 4, we present several numerical experiments to demonstrate the accuracy and efficiency of our algorithm. Finally, in Section 5, we give some concluding remarks.

## II. WEAK FORM AND DISCRETE FORM

In this paper, we consider the following second-order

eigenvalue problem:

$$\begin{cases} -\Delta u(x, y) + \alpha u(x, y) = \lambda u(x, y), & \text{in } \Omega, \\ u(x, y) = 0, & \text{on } \partial\Omega, \end{cases} \quad (2.1)$$

where  $\alpha$  is a non-negative constant,  $\Omega \in \mathbb{R}^2$  is a two-dimensional complex sectoral region. Following [18], the polar coordinate transformation is defined as follows:

$$x = r\delta(\theta) \cos \theta, \quad y = r\delta(\theta) \sin \theta, \quad 0 < a < r < b, \quad 0 \leq \theta_1 < \theta < \theta_2 \leq 2\pi, \quad (2.2)$$

here  $\delta(\theta)$  is a function related to the angle  $\theta$ .

Applying (2.2) and performing a direct computation, we obtain

$$\begin{aligned} \partial_x^2 u + \partial_y^2 u &= \frac{1}{r} \frac{1}{\delta^2} \left\{ \left[ 1 + \frac{(\partial_\theta \delta)^2}{\delta^2} \right] \partial_r (r \partial_r \tilde{u}) + \frac{1}{r} \partial_\theta^2 \tilde{u} \right. \\ &\quad \left. - \partial_r \left( \frac{\partial_\theta \delta}{\delta} \partial_\theta \tilde{u} \right) - \partial_\theta \left( \frac{\partial_\theta \delta}{\delta} \partial_r \tilde{u} \right) \right\} =: \Delta_p \tilde{u}, \end{aligned}$$

where  $\tilde{u}(r, \theta) = u(r\delta(\theta) \cos \theta, r\delta(\theta) \sin \theta)$ . Then, (2.1) can be rewritten as follows:

$$\begin{cases} -\Delta_p \tilde{u}(r, \theta) + \alpha \tilde{u}(r, \theta) = \lambda \tilde{u}(r, \theta), & (r, \theta) \in (a, b) \times (\theta_1, \theta_2), \\ \tilde{u}(a, \theta) = \tilde{u}(b, \theta) = 0, & \theta \in (\theta_1, \theta_2), \\ \tilde{u}(r, \theta_1) = \tilde{u}(r, \theta_2) = 0, & r \in (a, b). \end{cases} \quad (2.3)$$

Let

$$\begin{aligned} r &= \frac{a+b}{2} + \frac{b-a}{2}t, \quad \theta = \frac{\theta_1 + \theta_2}{2} + \frac{\theta_2 - \theta_1}{2}\varsigma, \\ (t, \varsigma) &\in \mathcal{D} = [-1, 1] \times [-1, 1], \\ \hat{u}(t, \varsigma) &= \tilde{u}\left(\frac{a+b}{2} + \frac{b-a}{2}t, \frac{\theta_1 + \theta_2}{2} + \frac{\theta_2 - \theta_1}{2}\varsigma\right), \\ \rho(\varsigma) &= \delta\left(\frac{\theta_1 + \theta_2}{2} + \frac{\theta_2 - \theta_1}{2}\varsigma\right). \end{aligned}$$

Then, one obtains

$$\begin{aligned} \Delta_p \tilde{u} &= \frac{2}{[(a+b) + (b-a)t]\rho^2} \left\{ \frac{2}{b-a} \left( 1 + \frac{4}{(\theta_2 - \theta_1)^2} \frac{(\partial_\varsigma \rho)^2}{\rho^2} \right) \right. \\ &\quad \left[ \partial_t \hat{u} + \left( t + \frac{b+a}{b-a} \partial_t^2 \hat{u} \right) \right] + \frac{8}{[a+b + (b-a)t](\theta_2 - \theta_1)^2} \partial_\varsigma^2 \hat{u} \right. \\ &\quad \left. - \frac{8}{(b-a)(\theta_2 - \theta_1)^2} \left[ \partial_t \left( \frac{\partial_\varsigma \rho}{\rho} \partial_\varsigma \hat{u} \right) + \partial_\varsigma \left( \frac{\partial_\varsigma \rho}{\rho} \partial_t \hat{u} \right) \right] \right\} =: L_p \hat{u}. \end{aligned}$$

Then, (2.3) can be restated as follows:

$$\begin{cases} -L_p \hat{u} + \alpha \hat{u} = \lambda \hat{u}, & (t, \varsigma) \in \mathcal{D}, \\ \hat{u}(\pm 1, \varsigma) = \hat{u}(t, \pm 1) = 0, & \varsigma, t \in [-1, 1]. \end{cases} \quad (2.4)$$

Next, in order to derive the weak form of equation (2.4) and its discrete scheme. We first define the following Sobolev spaces:

$$\begin{aligned} \mathcal{H}_*^1(\mathcal{D}) &= \{p: \int_{\mathcal{D}} |\partial_t p|^2 + \left| \frac{\partial_\varsigma \rho}{\rho} \partial_t p - \partial_\varsigma p \right|^2 dt d\varsigma \\ &\quad < \infty, p(t, \pm 1) = 0, p(\pm 1, \varsigma) = 0\}, \end{aligned}$$

and the corresponding inner product and norm are given by

$$\begin{aligned} (p, q)_{1,*} &= \int_{\mathcal{D}} \left( 1 + \frac{1}{\vartheta^2} \frac{(\partial_\varsigma \rho)^2}{\rho^2} \right) \partial_t p \partial_t q - \frac{1}{\vartheta} \frac{\partial_\varsigma \rho}{\rho} (\partial_t p \partial_\varsigma q \\ &\quad + \partial_\varsigma p \partial_t q) + \partial_\varsigma p \partial_\varsigma q dt d\varsigma, \\ \|p\|_{1,*} &= \left( \int_{\mathcal{D}} |\partial_t p|^2 + \left| \frac{\partial_\varsigma \rho}{\rho} \partial_t p - \partial_\varsigma p \right|^2 dt d\varsigma \right)^{\frac{1}{2}}, \end{aligned}$$

$$\vartheta = \frac{\theta_2 - \theta_1}{2}.$$

Then, using boundary conditions and integration by parts, we immediately get the variational formulation of (2.4), which can be formulated as follows: Find  $(\lambda, \hat{u}) \in \mathbb{R} \times \mathbf{H}_*^1(\mathcal{D})$ , such that

$$\mathbf{A}(\hat{u}, \hat{v}) = \lambda \mathbf{B}(\hat{u}, \hat{v}), \quad \forall \hat{v} \in \mathbf{H}_*^1(\mathcal{D}), \quad (2.5)$$

where

$$\begin{aligned} \mathcal{A}(\hat{u}, \hat{v}) &= \frac{\theta_2 - \theta_1}{2(b-a)} \int_{\mathcal{D}} [a+b + (b-a)t] \left( 1 + \frac{4}{(\theta_2 - \theta_1)^2} \frac{(\partial_\varsigma \rho)^2}{\rho^2} \right) \partial_t \hat{u} \partial_t \hat{v} dt d\varsigma \\ &\quad + \frac{2(b-a)}{\theta_2 - \theta_1} \int_{\mathcal{D}} \frac{1}{a+b + (b-a)t} \partial_\varsigma \hat{u} \partial_\varsigma \hat{v} dt d\varsigma \\ &\quad - \frac{2}{\theta_2 - \theta_1} \int_{\mathcal{D}} \frac{\partial_\varsigma \rho}{\rho} \partial_t \hat{u} \partial_\varsigma \hat{v} dt d\varsigma - \frac{2}{\theta_2 - \theta_1} \int_{\mathcal{D}} \frac{\partial_\varsigma \rho}{\rho} \partial_\varsigma \hat{u} \partial_t \hat{v} dt d\varsigma \\ &\quad + \alpha \frac{(b-a)(\theta_2 - \theta_1)}{8} \int_{\mathcal{D}} [a+b + (b-a)t] \rho^2 \hat{u} \hat{v} dt d\varsigma, \\ \mathcal{B}(\hat{u}, \hat{v}) &= \frac{(b-a)(\theta_2 - \theta_1)}{8} \int_{\mathcal{D}} [a+b + (b-a)t] \rho^2 \hat{u} \hat{v} dt d\varsigma. \end{aligned}$$

Let  $P_N$  be the space of polynomials of degree less than or equal to  $N$  and define the approximation space:  $X_N = (P_N \times P_N) \cap \mathbf{H}_*^1(\mathcal{D})$ . Then, a Legendre-Galerkin spectral approximation associated with (2.5) is: Find  $(\lambda_N, \hat{u}_N) \in \mathbb{R} \times X_N$ , such that

$$\mathbf{A}(\hat{u}_N, \hat{v}_N) = \lambda_N \mathbf{B}(\hat{u}_N, \hat{v}_N), \quad \forall \hat{v}_N \in X_N. \quad (2.6)$$

### III. ALGORITHM DESIGN OF THE DISCRETE SCHEME

In this section, we will describe the implementation process of the algorithm in detail. We first construct a set of basis functions for the approximation space  $X_N$ . Denote by

$L_i(t)$  the Legendre polynomial of degree  $i$ . Let

$$\varphi_i(t) = L_i(t) - L_{i+2}(t), \quad (i = 0, 1, \dots, N-2),$$

$$X_N = \text{span}\{\varphi_i(t)\varphi_j(\varsigma), i, j = 0, \dots, N-2\}, \quad I = (-1, 1).$$

Let us denote

$$\begin{aligned} a_{im} &= \frac{\theta_2 - \theta_1}{2(b-a)} \int_I [a+b + (b-a)t] \varphi_i' \varphi_m' dt, \\ b_{jn} &= \int_I \left( 1 + \frac{4}{(\theta_2 - \theta_1)^2} \frac{(\partial_\varsigma \rho)^2}{\rho^2} \right) \varphi_j \varphi_n d\varsigma, \\ c_{im} &= \int_I \frac{1}{a+b + (b-a)t} \varphi_i \varphi_m dt, \quad d_{jn} = \frac{2(b-a)}{\theta_2 - \theta_1} \int_I \varphi_j' \varphi_n' d\varsigma, \\ e_{im} &= \frac{2}{\theta_2 - \theta_1} \int_I \varphi_i \varphi_m' dt, \quad f_{jn} = \int_I \frac{\partial_\varsigma \rho}{\rho} \varphi_j' \varphi_n d\varsigma, \\ g_{im} &= \frac{2}{\theta_2 - \theta_1} \int_I \varphi_i' \varphi_m dt, \quad h_{jn} = \int_I \frac{\partial_\varsigma \rho}{\rho} \varphi_j \varphi_n' d\varsigma, \\ k_{im} &= \int_I [a+b + (b-a)t] \varphi_i \varphi_m dt, \end{aligned}$$

$$p_{jn} = \frac{(b-a)(\theta_2 - \theta_1)}{8} \int_I \rho^2 \varphi_j \varphi_n d\zeta.$$

We expand the eigenfunction  $\hat{u}_N$  as follows:

$$\hat{u}_N = \sum_{i,j=0}^{N-2} u_{ij} \varphi_i(t) \varphi_j(\zeta), \quad (3.1)$$

where  $u_{ij}$  is the expansion coefficient.

Denote

$$U = \begin{pmatrix} u_{00} & u_{01} & \cdots & u_{0N-2} \\ u_{10} & u_{11} & \cdots & u_{1N-2} \\ \vdots & \vdots & \ddots & \vdots \\ u_{N-20} & u_{N-21} & \cdots & u_{N-2N-2} \end{pmatrix}.$$

We use  $\bar{U}$  to denote the vector formed by the columns of  $U$ .

Now, plugging the expressions of (3.1) in (2.6), and taking  $\hat{v}_N$  through all the basis functions in  $X_N$ , we obtain

$$\begin{aligned} \mathcal{A}(\hat{u}_N, \hat{v}_N) &= \sum_{i,j=0}^{N-2} \frac{\theta_2 - \theta_1}{2(b-a)} \int_D [a+b+(b-a)t] (1 \\ &\quad + \frac{4}{(\theta_2 - \theta_1)^2} \frac{(\partial_\zeta \rho)^2}{\rho^2}) \varphi_i' \varphi_j \varphi_m' \varphi_n dtd\zeta u_{ij} \\ &+ \sum_{i,j=0}^{N-2} \frac{2(b-a)}{\theta_2 - \theta_1} \int_D \frac{1}{a+b+(b-a)t} \varphi_i \varphi_j' \varphi_m \varphi_n' dtd\zeta u_{ij} \\ &- \sum_{i,j=0}^{N-2} \frac{2}{\theta_2 - \theta_1} \int_D \frac{\partial_\zeta \rho}{\rho} (\varphi_i \varphi_j' \varphi_m' \varphi_n + \varphi_i' \varphi_j \varphi_m \varphi_n') dtd\zeta u_{ij} \\ &+ \alpha \sum_{i,j=0}^{N-2} \frac{(b-a)(\theta_2 - \theta_1)}{8} \int_D [a+b+(b-a)t] \rho^2 \varphi_i \varphi_j \varphi_m \varphi_n dtd\zeta u_{ij}, \\ &= (A(n,:) \otimes B(m,:) + C(n,:) \otimes D(m,:) - E(n,:) \otimes F(m,:)) \\ &\quad - G(n,:) \otimes H(m,:) + \alpha K(n,:) \otimes P(m,:)) \bar{U}, \end{aligned}$$

and

$$\begin{aligned} \mathcal{B}(\hat{u}_N, \hat{v}_N) &= \sum_{i,j=0}^{N-2} \frac{(b-a)(\theta_2 - \theta_1)}{8} \int_D [a+b+(b-a)t] \rho^2 \varphi_i \varphi_j \varphi_m \varphi_n dtd\zeta u_{ij} = K(n,:) \otimes P(m,:) \bar{U}, \text{ where} \\ A &= (a_{im}), B = (b_{jn}), C = (c_{im}), D = (d_{jn}), E = (e_{im}), \\ F &= (f_{jn}), G = (g_{im}), H = (f_{jn}), K = (k_{im}), P = (p_{jn}), \end{aligned}$$

and  $\otimes$  represents the tensor product symbol of the matrix,

$A(n,:)$  represents the  $n$ -th row of matrix  $A$ . Let

$$A = A(n,:) \otimes B(m,:) + C(n,:) \otimes D(m,:) - E(n,:) \otimes F(m,:) - G(n,:) \otimes H(m,:) + \alpha K(n,:) \otimes P(m,:), B = K(n,:) \otimes P(m,:).$$

Then, we can obtain the equivalent matrix form of the discrete variational form (2.6) as follows:

$$A\bar{U} = \lambda_N B\bar{U}. \quad (3.2)$$

#### IV. NUMERICAL EXPERIMENTS

In this section, we will use two numerical examples on the MATLAB R2018b platform to verify that the algorithm we proposed earlier is a high-precision numerical method. It should be particularly noted that the expression of  $\delta(\theta)$  largely determines the complexity of the region. Without loss of generality, in the following two examples, we set  $\delta(\theta) = (\sin^4 \theta + \cos^4 \theta)^{\frac{1}{4}}$ .

**Example 1:** We take  $\alpha = \beta = 1, \theta_1 = 0, \theta_2 = \frac{\pi}{2}, a = \frac{1}{2}, b = 1$ . The numerical results of the first fourth eigenvalues  $\lambda_N^j (j = 1, 2, 3, 4)$  for different  $N$  are listed in Table 1. To intuitively demonstrate the spectral accuracy of our algorithm, we use the numerical solution with  $N=60$  as a reference solution and plot the absolute error curves of approximate eigenvalues as well as corresponding error curves under a log-log scale in Figure 1. Additionally, Figure 2 provides an image of the reference solution for the eigenfunction and an error image between the reference solution and the approximate solution with  $N = 50$ .

TABLE 1. The first four approximation eigenvalues for different  $N$

$N$	$\lambda_N^1$	$\lambda_N^2$	$\lambda_N^3$	$\lambda_N^4$
2	38.606182916	61.414558470	87.952727599	125.98742961
0	85105	73811	61485	91142
3	38.606182581	61.414555727	87.952723504	125.987366886
0	18772	20928	61916	83963
4	38.606182581	61.414555726	87.952723503	125.987366886
0	05261	29643	63464	15286
5	38.606182581	61.414555726	87.952723503	125.987366886
0	05275	29592	63491	15256

From Table 1, it can be observed that as  $N$  increases, the number of significant digits of the approximate eigenvalues also increases continuously, indicating that the proposed algorithm in this paper exhibits excellent convergence. When  $N \geq 40$ , the first four eigenvalues achieve at least 12-digit accuracy, fully validating the high-precision characteristics of the algorithm. In addition, as shown in Figures 1-2, our algorithm is both convergent and spectral accurate.

**Example 2.** We take  $\theta_1 = 0, \theta_2 = \pi, a = \frac{1}{2}, b = 1$  and  $\alpha = 1$ .

The numerical results of the first fourth eigenvalues  $\lambda_N^j (j = 1, 2, 3, 4)$  for different  $N$  are listed in Table 2. We use the numerical solution with  $N=120$  as a reference solution and plot the absolute error curves of approximate eigenvalues as well as corresponding error curves under a log-log scale in Figure 3. Additionally, Figure 4 provides an image of the reference solution for the eigenfunction and an error image between the reference solution and the approximate solution with  $N=100$ .

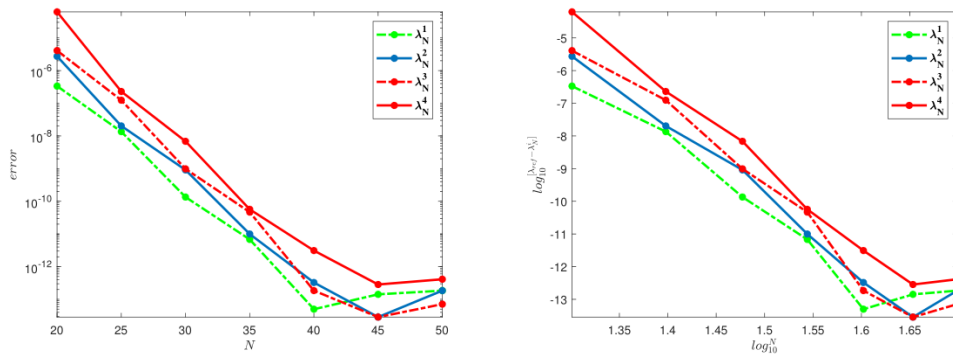


Figure 1: Absolute error curves (left) between the numerical solution and the reference solution and the errors curves (right) under log-log scale.

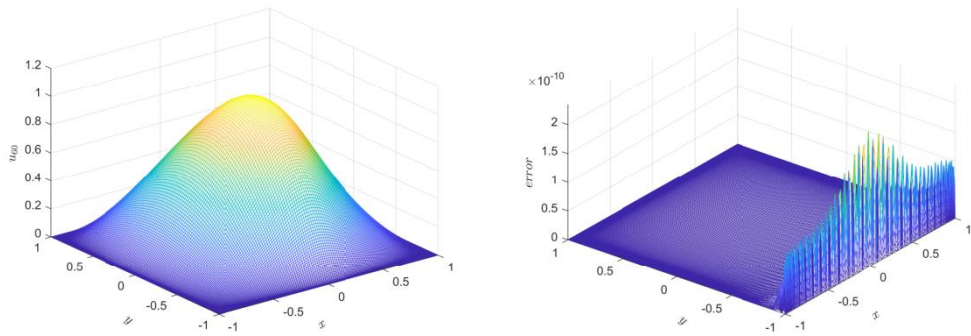


Figure 2: Image (left) of the reference solution  $u_{60}(x, y)$  and the error image (right) between reference solution and numerical solution  $u_{50}(x, y)$ .

TABLE 2. The first four approximation eigenvalues for different  $N$

$N$	$\lambda_N^1$	$\lambda_N^2$	$\lambda_N^3$	$\lambda_N^4$
40	44.95027972545694	58.79680548274361	91.41616546541546	136.8474904345504
60	44.95027693348787	58.79680125027318	91.41616248371694	136.8474819414608
80	44.95027692871246	58.79680124277311	91.41616247896927	136.8474819251731
100	44.95027692870467	58.79680124274616	91.41616247895206	136.8474819251479

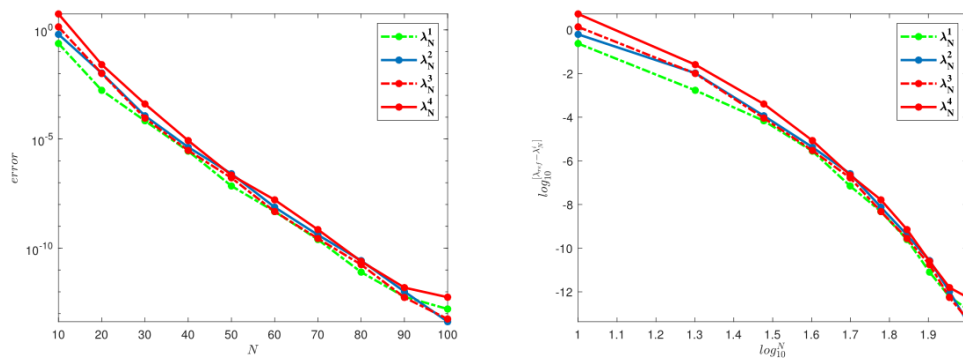


Figure 3: Absolute error curves (left) between the numerical solution and the reference solution and the errors curves (right) under log-log scale.

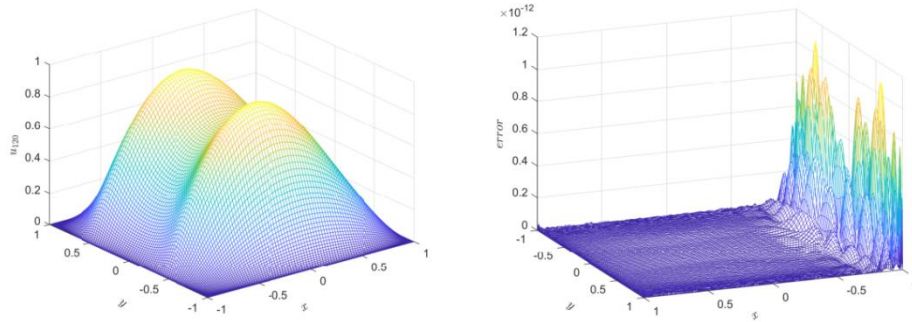


Figure 4: Image (left) of the reference solution  $u_{120}(x, y)$  and the error image (right) between reference solution and numerical solution  $u_{110}(x, y)$ .

We observe from Table 2 that the first four eigenvalues achieve at least 11-digit accuracy with  $N \geq 100$ . Again, as shown in Figures 3-4, our algorithm is both convergent and spectral accurate.

### V. CONCLUSION

In this paper, we develop a Legendre-Galerkin spectral method for solving second-order eigenvalue problems in complex domains. By means of polar and affine transformations, we map the complex sector region into a regular rectangular domain on which the weak formulation and its corresponding discrete variational form are established. In addition, the numerical calculation results verify the effectiveness and high accuracy of the algorithm.

### REFERENCES

- [1] Cakoni F, Colton D, Monk P. Iterative Methods for Transmission Eigenvalue Problems. *SIAM J. Numer. Anal.*, 2014, 52(1): 160-181.
- [2] Tikhonov, A. N., A. A. Samarskii *Boundary and eigenvalue problems in mathematical physics.* New York: Dover Publications, 1963.
- [3] Fletcher, C. A. J. *Eigenvalue problems in physics and engineering.* Springer, 1984.
- [4] W. Chen, Q. Lin. Approximation of an Eigenvalue Problem Associated with the Stokes Problem by the Stream Function-Vorticity-Pressure Method. *Applications of Mathematics*, 2006, 51(1): 73-88.
- [5] J. Shen. Efficient spectral-Galerkin methods III: Polar and cylindrical geometries. *SIAM J. Sci. Comput.*, 1997, 18(6): 1583-1604.
- [6] J. An, H. Y. Li, Z. M. Zhang. Spectral-Galerkin approximation and optimal error estimate for biharmonic eigenvalue problems in circular/spherical/elliptical domains. *Numer. Algorithms*, 2020, 84(2): 427-455.
- [7] H. Y. Li, Y. Xu. Spectral approximation on the unit ball. *SIAM J. Numer. Anal.*, 2014, 52(6): 2647-2675.
- [8] J. An, Z. M. Zhang. An efficient spectral-Galerkin approximation and error analysis for Maxwell transmission eigenvalue problems in spherical geometries. *J. Sci. Comput.*, 2018, 75(1): 157-181.
- [9] M. Zheng, F. Liu, I. Turner, V. Anh. A novel high order space-time spectral method for the time fractional Fokker-Planck equation. *SIAM Journal on Scientific Computing*, 2015, 37(2): A701-A724.
- [10] J. Hu, X. Huang, J. Shen, H. Yang. A fast Petrov-Galerkin spectral method for the multidimensional Boltzmann equation using mapped Chebyshev functions. *SIAM Journal on Scientific Computing*, 2022, 44(3): A1497-A1524.
- [11] Yadykin. I.B., Galyaev, I.A. Structural Spectral Methods of Solving Continuous Generalized Lyapunov Equation. *Autom Remote Control*, 2024, 85: 835-842.
- [12] M. Xia, X. Li, Q. Shen. Learning unbounded-domain spatiotemporal differential equations using adaptive spectral methods. *J. Appl. Math. Comput.*, 2024, 70: 4395-4421.
- [13] Y. Q. Gu, J. Shen. Accurate and efficient spectral methods for elliptic PDEs in complex domains. *J. Sci. Comput.*, 2020, 83: 1-20.
- [14] Y.Q. Gu, J. Shen. An efficient spectral method for elliptic PDEs in complex domains with circular embedding. *SIAM J. Sci. Comput.*, 2021, 43(1): A309-A329.
- [15] Y. Q. Gu, J. Shen. A fictitious domain spectral method for solving the Helmholtz equation in exterior domains. *J. Sci. Comput.*, 2023, 94(46): 1-27.
- [16] S. H. Lui. Spectral domain embedding for elliptic PDEs in complex domains. *J. Comput. Appl. Math.*, 2009, 225(2): 541-557.
- [17] S. A. Orszag. Spectral methods for problems in complex geometries. *J. Chem. Phys.*, 1980, 37: 70-92.
- [18] Z. Q. Wang, X. Wen, G. Q. Yao. An efficient spectral-Galerkin method for elliptic equations in 2D complex geometries. *J. Sci. Comput.*, 2023, 95(89): 1-26.